British Journal of Pharmacology

DOI:10.1111/bph.13068
www.brjpharmacol.org

Themed Section: Chinese Innovation in Cardiovascular Drug Discovery

RESEARCH PAPER

Cryptotanshinone, an orally bioactive herbal compound from Danshen, attenuates atherosclerosis in apolipoprotein E-deficient mice: role of lectin-like oxidized LDL receptor-1 (LOX-1)

Zhiping Liu[1,2], Suowen Xu[1,3], Xiaoyang Huang[1], Jiaojiao Wang[1], Si Gao[1], Hong Li[1], Changhua Zhou[1], Jiantao Ye[1], Shaorui Chen[1], Zheng-Gen Jin[3] and Peiqing Liu[1]

[1]*Department of Pharmacology and Toxicology, National and Local United Engineering Lab of Druggability and New Drugs Evaluation, Guangdong Provincial Key Laboratory of Construction Foundation, School of Pharmaceutical Sciences, Sun Yat-sen University, Guangzhou, China,* [2]*Drug Discovery Center, School of Chemical Biology and Biotechnology (SCBB), Shenzhen Graduate School of Peking University, Shenzhen, China, and* [3]*Aab Cardiovascular Research Institute, School of Medicine and Dentistry, University of Rochester, Rochester, NY, USA*

Correspondence
Peiqing Liu, Department of Pharmacology and Toxicology, School of Pharmaceutical Sciences, Sun Yat-sen University (Higher Education Mega Center), 132# East Wai-huan Road, Guangzhou, 510006 Guangdong, China. E-mail: liupq@mail.sysu.edu.cn

Zhiping Liu and Suowen Xu contributed equally to this work.

Received
23 December 2014
Accepted
24 December 2014

BACKGROUND AND PURPOSE

Cryptotanshinone (CTS) is a major bioactive diterpenoid isolated from Danshen, an eminent medicinal herb that is used to treat cardiovascular disorders in Asian medicine. However, it is not known whether CTS can prevent experimental atherosclerosis. The present study was designed to investigate the protective effects of CTS on atherosclerosis and its molecular mechanisms of action.

EXPERIMENTAL APPROACH

Apolipoprotein E-deficient ($ApoE^{-/-}$) mice, fed an atherogenic diet, were dosed daily with CTS (15, 45 mg kg^{-1} day^{-1}) by oral gavage. *In vitro* studies were carried out in oxidized LDL (oxLDL)-stimulated HUVECs treated with or without CTS.

KEY RESULTS

CTS significantly attenuated atherosclerotic plaque formation and enhanced plaque stability in $ApoE^{-/-}$ mice by inhibiting the expression of lectin-like oxLDL receptor-1 (LOX-1) and MMP-9, as well as inhibiting reactive oxygen species (ROS) generation and NF-κB activation. CTS treatment significantly decreased the levels of serum pro-inflammatory mediators without altering the serum lipid profile. *In vitro*, CTS decreased oxLDL-induced LOX-1 mRNA and protein expression and, thereby, inhibited LOX-1-mediated adhesion of monocytes to HUVECs, by reducing the expression of adhesion molecules (intracellular adhesion molecule 1 and vascular cellular adhesion molecule 1). Furthermore, CTS inhibited NADPH oxidase subunit 4 (NOX4)-mediated ROS generation and consequent activation of NF-κB in HUVECs.

CONCLUSIONS AND IMPLICATIONS

CTS was shown to have anti-atherosclerotic activity, which was mediated through inhibition of the LOX-1-mediated signalling pathway. This suggests that CTS is a vasculoprotective drug that has potential therapeutic value for the clinical treatment of atherosclerotic cardiovascular diseases.

LINKED ARTICLES

This article is part of a themed section on Chinese Innovation in Cardiovascular Drug Discovery. To view the other articles in this section visit http://dx.doi.org/10.1111/bph.2015.172.issue-23

Abbreviations

ApoE$^{-/-}$, apolipoprotein E deficient; CD36, cluster of differentiation 36; CTS, cryptotanshinone; HCD, high cholesterol diet; ICAM-1, intracellular adhesion molecule 1; LOX-1, lectin-like oxidized low-density lipoprotein receptor-1; NOX4, NADPH oxidase subunit 4; oxLDL, oxidized low-density lipoprotein; ROS, reactive oxygen species; SMCs, smooth muscle cells; SR-A, scavenger receptor-A; VCAM-1, vascular cellular adhesion molecule 1

Tables of Links

TARGETS
Nuclear hormone receptors[a]
PPARγ
Enzymes[b]
MMP-9

LIGANDS		
Angiotensin II	IFN-γ	IL-17A
Homocysteine	IL-1β	TNF-α
ICAM-1	IL-6	VCAM-1

These Tables list key protein targets and ligands in this article which are hyperlinked to corresponding entries in http://www.guidetopharmacology.org, the common portal for data from the IUPHAR/BPS Guide to PHARMACOLOGY (Pawson *et al.*, 2014) and are permanently archived in the Concise Guide to PHARMACOLOGY 2013/14 ([a,b]Alexander *et al.*, 2013a,b).

Introduction

Atherosclerotic cardiovascular disease, driven and regulated by lipid retention (in the artery wall), lipid oxidation, persistent inflammation and immune response disturbances, is the leading cause of premature death in developed and developing countries (Ross, 1999; Libby *et al.*, 2013). One critical event in the initiation of atherosclerosis is the adhesion of leukocytes to activated endothelium and their subsequent migration into the vessel wall. These cellular processes are mediated by the up-regulation of adhesion molecules in endothelial cells (ECs) and an increased expression of leukocyte chemotactic factors in the vascular wall (Libby, 2002). One major determinant of this alteration could be oxidative stress. Modified LDL, in particular oxidized LDL (oxLDL; the pathological form of oxidatively modified LDL), exerts several pro-atherogenic effects to facilitate atherosclerosis (Li and Glass, 2002). The plasma oxLDL level is transiently increased before the development of atherosclerotic lesions in apolipoprotein E-deficient (ApoE$^{-/-}$) mice (Kato *et al.*, 2009), suggesting that oxLDL may play a crucial role in the early stages in the formation of atherosclerotic lesions. Previous studies have shown that lectin-like oxLDL receptor-1 (LOX-1), a primary scavenger receptor expressed in ECs (Sawamura *et al.*, 1997), is up-regulated in atherosclerotic plaques of experimental animals and humans (Kataoka *et al.*, 1999). LOX-1 facilitates the uptake of oxLDL by ECs and macrophages, thus mediating several of its biological effects (Li *et al.*, 2003; Li and Mehta, 2009; Xu *et al.*, 2012; 2013b): oxLDL induces (i) apoptosis of ECs and phagocytosis of aged and apoptotic cells; (ii) the adhesion of monocytes to activated endothelium; and (iii) macrophage-derived foam cell formation. More recently, it has been demonstrated that LOX-1 is the main culprit that transduces the signal of the adverse effects of dysfunctional high-density lipoprotein (HDL; such as oxidized HDL and HDL from patients with coronary artery disease) (Besler *et al.*, 2011). *In vitro*, LOX-1 expression is up-regulated by various pro-atherogenic stimuli, including oxLDL, TNF-α, angiotensin II, shear stress, homocysteine and high glucose (Xu *et al.*, 2013b). Therefore, LOX-1 has recently been suggested as an attractive therapeutic target for atherosclerosis (Xu *et al.*, 2013b).

Danshen (*Salvia miltiorrhiza* Bunge) is a versatile traditional Chinese medicine that has been widely used in Asian countries for the treatment of cardiovascular diseases (Gao *et al.*, 2012). To date, over 90 kinds of constituents from Danshen have been reported. Of these phytochemicals, tanshinones are a group of lipophilic abietane diterpene compounds that include tanshinone I, tanshinone IIA (TSN), cryptotanshinone (CTS), dihydrotanshinone I and so on. As the most abundant and bioactive constituents from Danshen, TSN and CTS, by modifying numerous signalling pathways, have demonstrated therapeutic effects in many diseases (Xu

and Liu, 2013a). Recent work from our laboratory has demonstrated that TSN exerts a potent anti-atherogenic effect in hyperlipidaemic rabbits (Chen *et al.*, 2012), rats (Tang *et al.*, 2007) and ApoE$^{-/-}$ mice (Tang *et al.*, 2011a; Xu *et al.*, 2011; Liu *et al.*, 2014). CTS, another major tanshinone compound isolated from Danshen, is structurally very similar to TSN except for the C-15 position of the dihydrofuran ring (Supporting Information Fig. S1). Reports from our laboratory and others have demonstrated that CTS possesses potent anti-oxidative, anti-inflammatory and immunomodulatory properties, contributing to its therapeutic effects on neurodegenerative diseases (Mei *et al.*, 2009; 2012), diabetes (Kim *et al.*, 2007) and cancers (Shin *et al.*, 2009; Chen *et al.*, 2010). However, there is no report on the potential anti-atherosclerotic effects of CTS *in vivo*.

Therefore, in the present study, we investigated the potential effects of CTS on atherosclerotic plaque development in ApoE$^{-/-}$ mice kept on a high cholesterol diet (HCD). Additionally, we examined the modulation of LOX-1 expression by CTS in HUVECs stimulated with oxLDL.

Methods

Preparation of CTS

CTS was kindly provided by Professor Lianquan Gu at the Department of Chemistry, School of Pharmaceutical Sciences, Sun Yat-sen University (Guangzhou, China). The structure of the compound was established based on MS and NMR data and by comparison with those of an authentic sample. The chemical purities of CTS were >98% as judged by HPLC. In animal experiments, we prepared a complex of CTS with hydroxypropyl-β-cyclodextrin in order to improve the bioavailability of CTS *in vivo* as described previously (Pan *et al.*, 2008).

Animal experiment

Experimental protocols were approved by the Animal Care and Use Committee of Sun Yat-sen University (Guangzhou, China). All animal experimental procedures were performed in accordance with the *Guide for the Care and Use of Laboratory Animals* (NIH Publication, revised 1999, No. 3040-2, Bethesda, MD, USA). All studies involving animals are reported in accordance with the ARRIVE guidelines for reporting experiments involving animals (Kilkenny *et al.*, 2010; McGrath *et al.*, 2010). Male ApoE$^{-/-}$ mice on C57BL/6J background and age-matched wild-type C57BL/6J controls were purchased from Peking University Experimental Animal Center (Beijing, China). The mice were housed under a 12-h light/dark cycle in specific pathogen-free facility at Institutional Experimental Animal Center. Starting from 6 weeks, the mice were fed with a HCD (10% fat, 1.25% cholesterol, 0% cholic acid) for 16 weeks. All ApoE$^{-/-}$ mice were dosed daily via intragastric gavage with 15 or 45 mg kg^{-1} CTS dissolved in 0.5% carboxy-methyl-cellulose sodium (CMC-Na) or administered 0.5% CMC-Na alone (vehicle control) (n = 10 per group). The dose of CTS used in this study was based on previous reports of its effectiveness in animals with Alzheimer's disease and acute lung injury (Mei *et al.*, 2009; Tang *et al.*, 2014). Ten male age-matched C57BL/6J mice were used as a control group; they were treated with the vehicle for CTS. All animals received food and water *ad libitum*. Body weight and food intake were monitored during the study.

Histology and immunohistochemistry

Aortic sinus morphometric and immunohistochemical analysis was performed as described previously in detail (Xu *et al.*, 2011). Sections of 8 μm thickness were used for immunohistochemical staining with CD68 (Boster, Wuhan, China), LOX-1 and NF-κB p65 antibodies (Abcam, Cambridge, MA, USA). Colour reaction was developed with diaminobenzidine (Sigma-Aldrich, St. Louis, MO, USA). For immunohistochemical analysis, sections of each aortic sinus were stained with MMP-9 (Abcam) and α-smooth muscle actin (α-SMA; Boster). The remainders of the sections were utilized for hematoxylin-eosin (H&E) staining to examine basic lesion morphology and Masson' trichrome staining for collagen.

Detection of serum lipid profile and pro-inflammatory cytokines

For measurement of the lipids, blood samples were collected at baseline (6 week) and the end of the diet treatment period (22 week), by retro-orbital venous plexus bleeding, from animals that had been fasted overnight. Serum total cholesterol, HDL cholesterol, LDL cholesterol and triglycerides were measured by colorimetric assays as previously described (Xu *et al.*, 2011). Serum pro-inflammatory cytokines were detected using Bio-Plex Pro Mouse Cytokine Assay Kit (Bio-Rad, Hercules, CA, USA) according to the manufacturer's protocol.

Morphometric analysis of atherosclerotic lesions

The *en face* and aortic sinus cryosection techniques (Xu *et al.*, 2011) were used to quantify atherosclerosis development throughout the aorta as well as at the vessel origin. Oil Red O (ORO) staining was used to measure lesion area in *en face* aorta and aortic sinus. For quantitative analysis of the total lesion area in aortic sinus, eight separate cryosections (spacing 50 μm apart) from each mouse were manually analysed with the Leica Qwin PLUS Software (Leica Microsystems, Heidelberg, Germany). For plaque area in whole aorta, the percentage of ORO-positive stained area in relation to total luminal surface area was quantified using computer-assisted morphometry with NIH ImageJ software (http://imagej.nih.gov). Lesion size in the aortic sinus and *en face* arterial tree was measured by two observers blinded to experimental groups.

Reactive oxygen species (ROS) production in situ

The production of ROS in aortic root cryosections was assessed *in situ* by fluorescence microscopy of dihydroethidium (DHE)-stained sections as described, in detail, previously (Xu *et al.*, 2011). The fluorescence was quantified using NIH ImageJ software.

Cell culture

HUVECs were obtained from fresh umbilical cord veins from women with normal pregnancies, with patients' informed

consent, and cultured in Medium 199 supplemented with 20% FBS, 1% penicillin/streptomycin, 1% L-glutamine, 10 U mL^{-1} heparin and 25 μg mL^{-1} EC growth supplement. The cells were grown at 37°C in humidified 5% CO_2 and used for experiments between passages 3 and 5. The time of incubation and the concentration of drugs used are based on results from previous studies (Suh *et al.*, 2006; Ang *et al.*, 2011). CTS at a concentration from 1 to 10 μM had no significant effect on cell viability as determined by the MTT assay (data not shown).

Real-time PCR

Real-time PCR was conducted as previously described (Xu *et al.*, 2011). Sequences for the oligonucleotide primers used were designed with Primer 5.0 software (Premier Biosoft, Palo Alto, CA, USA) and were custom synthesized by Invitrogen (listed in Supporting Information Table S1). mRNA levels of target genes were measured by qRT-PCR and quantified with respect to the GAPDH housekeeping gene. The fold increase/decrease versus control cells presented was calculated by the $2^{-\Delta\Delta Ct}$ method (Livak and Schmittgen, 2001). Statistical differences between the treatment group and control group were subjected to Student's unpaired *t*-tests.

Western blot analysis

Western blot analyses were performed as previously described (Xu *et al.*, 2009). The levels of MMP-9, LOX-1, intracellular adhesion molecule 1 (ICAM-1), vascular cellular adhesion molecule 1 (VCAM-1) and NADPH oxidase subunit 4 (NOX4) were analysed with the following antibodies, respectively: rabbit anti-MMP-9 and LOX-1 antibody was purchased from Abcam. Rabbit anti-ICAM-1 and VCAM-1 antibodies were obtained from Epitomics (Burlingame, CA, USA). Rabbit anti-NOX4 antibody was from Upstate (Merck Millipore, Billerica, MA, USA). Mouse anti-α-tubulin antibody was purchased from Sigma-Aldrich. The densitometric intensities of the protein bands were analysed by Quantity-One software (Bio-Rad), and data are presented as the ratio of intensity of band of interest to that of α-tubulin.

Gelatin zymography

Rat aortic smooth muscle cells (SMCs) were pretreated with CTS for 3 h, then stimulated with oxLDL (80 μg mL^{-1}) for 24 h. The gelatinolytic activities of MMP-9 in conditioned media were evaluated as previously described (Xu *et al.*, 2011). The band intensities were analysed by Quantity-One software (Bio-Rad).

ROS production in HUVECs

The generation of ROS was monitored using the fluorescence of a DHE probe. Cells were pretreated with CTS for 3 h and then further incubated for 30 min with 10 μM DHE dye. Cells were then switched to serum-free medium containing 80 μg mL^{-1} oxLDL for 2 h. The fluorescence intensities were acquired at 540 nm excitation and 590 nm emission using high-content screening (Array Scan VT1, Thermo Scientific, Hudson, NH, USA).

In vitro *monocyte adhesion assay*

The human monocyte leukaemia cell line THP-1 was cultured in RPMI 1640 medium supplemented with 10% FBS and washed three times with PBS. Then THP-1 monocytes (10^6 cells mL^{-1}) in M199 medium were added to monolayers of HUVECs and incubated for 40 min. Non-adherent THP-1 cells were removed by washing four times with PBS. Attached cells were then observed by an inverted microscope with a 40× lens. The adhesion of monocytes to ECs was quantified by calculating the number of monocytes attached to ECs.

Electrophoretic mobility shift assay (EMSA)

NF-κB DNA binding activity was analysed by EMSA using the LightShift™ chemiluminescent EMSA kit (Pierce, Rockford, IL, USA). Nuclear extracts (4 μg) were incubated with a 3′ biotin-labelled NF-κB (5′-TGG AAA TGG GAA GTC TCA TAG GAC-3′) probe (consensus sequence underlined). The DNA/protein complex formed was separated from free oligonucleotides on 6% native PAGs (0.5× Tris/Borate/EDTA buffer at 100 V for 60 min). Chemiluminescent detection was performed using enhanced chemiluminescence reagents according to the vendor's protocols (Pierce). For cold competition experiments, 100-fold molar excess of unlabelled duplex oligonucleotides containing NF-κB consensus sequence was added to the nuclear extracts before incubation with the biotin-labelled oligonucleotides.

Luciferase reporter gene assay

NF-κB-dependent transcriptional activity was conducted as described, in detail, previously (Yu *et al.*, 2013). In brief, HUVECs were co-transfected with NF-κB reporter plasmid and pRL-TK as an internal control using jetPEI-HUVEC (Polyplus Transfections, Illkirch, France) according to the manufacturer's instructions. The luciferase activity was measured using the Dual-Luciferase Reporter Assay System (Promega, Madison, WI, USA) according to the manufacturer's protocol.

Statistical analysis

Thirty $ApoE^{-/-}$ mice were randomly allocated to groups and equal group sizes were obtained (n = 10 per group). Data are presented as mean ± SEM unless specified otherwise. Images shown are representative of five or more independent experiments. Statistical significance of differences was calculated using one-way ANOVA with Bonferroni *post hoc* for multiple group comparison or Student's unpaired *t*-test for two-group comparison where appropriate. The analyses were performed using GraphPad Prism Software version 5.02 (GraphPad Inc., La Jolla, CA, USA). A P value < 0.05 was considered to be statistically significant.

Results

CTS reduces atherosclerotic plaque development in $ApoE^{-/-}$ mice

We first examined the efficacy of CTS in diet-induced atherosclerosis in $ApoE^{-/-}$ mice. Notably, compared with vehicle control group, CTS treatment (15 and 45 mg kg^{-1} day^{-1}) significantly attenuated atherosclerotic lesion formation in the *en face* prepared aorta (Figure 1A and B) and aortic sinus (Figure 1C and D) of $ApoE^{-/-}$ mice fed a HCD for 16 weeks. Biochemical analysis of the lipid profile and serum pro-inflammatory cytokines indicates that CTS significantly

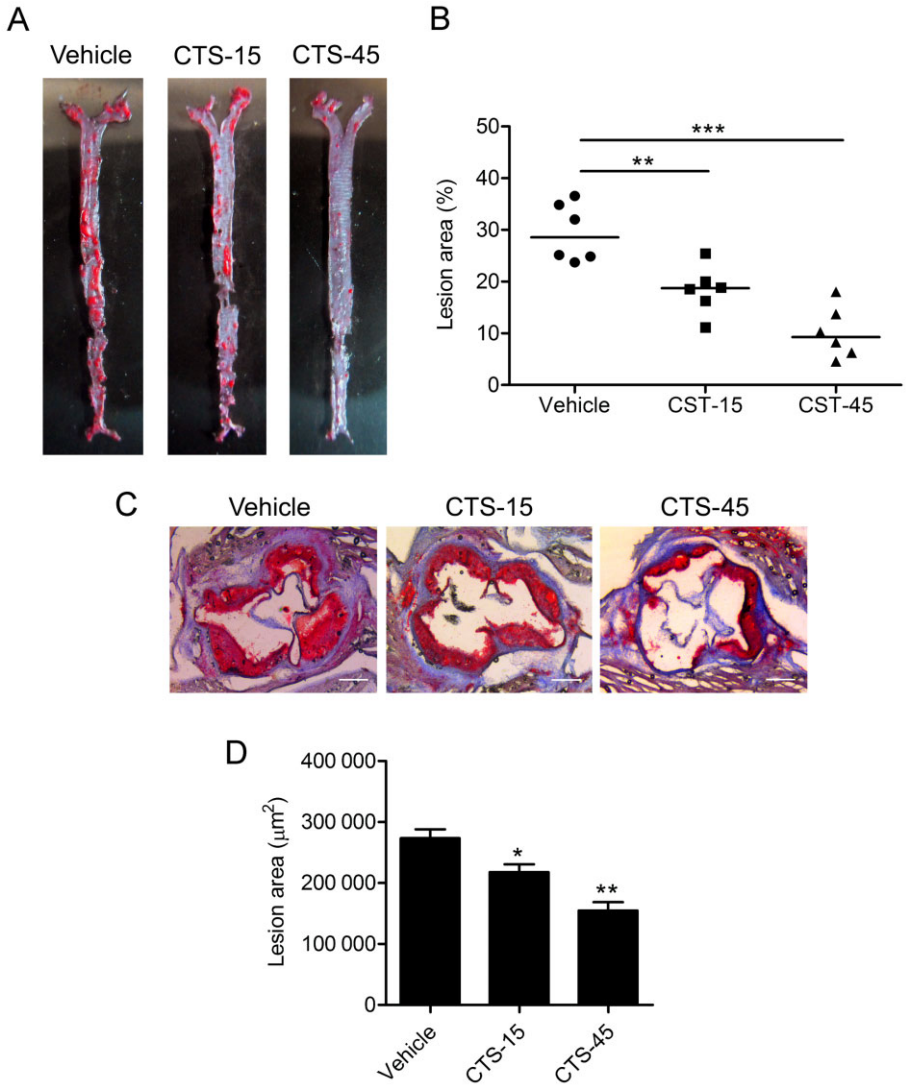

Figure 1

CTS attenuates atherosclerotic lesion size in ApoE$^{-/-}$ mice. (A) Atherosclerosis in the arterial tree was evaluated by Oil Red O staining. (B) Quantification of Oil Red O-positive areas in *en face* aorta by NIH ImageJ software. $n = 6$ for each group. (C) Representative photomicrographs of Oil Red O staining of the atherosclerotic lesions in the aortic sinus. Original magnification, ×50. (D) Morphometric analysis of atherosclerotic lesion size in aortic sinus. Average sizes of atherosclerotic lesions were calculated from eight sections in ApoE$^{-/-}$ mice fed an atherogenic diet. $n = 10$ for each group. *$P < 0.05$, **$P < 0.01$, ***$P < 0.001$ compared with vehicle group respectively.

reduced the serum levels of pro-inflammatory cytokines IL-1β, IL-6, IL-17A, IFN-γ and TNF-α (Table 1), without altering serum lipid levels (Supporting Information Table S2). These data suggest that CTS has potent anti-inflammatory and anti-atherosclerotic effects in experimental atherosclerosis independent of serum lipid levels.

CTS favours features of plaque stability in ApoE$^{-/-}$ mice

To further evaluate the effect of CTS on the biology of plaques, we analysed plaque composition in ApoE$^{-/-}$ mice. As shown in Figure 2A, atherosclerotic plaques in mice treated with CTS contained smaller necrotic core areas ($P < 0.01$ for CTS-15 group and $P < 0.001$ for CTS-45 group, compared with vehicle group). There was also a marked decrease in macrophage accumulation, as indicated by the immunostaining of the macrophage marker CD68 (Figure 2B) in atherosclerotic plaques of CTS-treated mice compared with vehicle-treated control mice. In contrast, a dramatic increase in collagen content, as determined by Masson' trichrome staining (Figure 2C), in atherosclerotic lesions from CTS-treated mice was observed.

MMP-9 is a crucial factor that determines atherosclerotic plaque instability. Therefore, we examined the effects of CTS on MMP-9 expression/activity. Interestingly, we did not observe any significant alterations in the expression or

Table 1

Serum levels of pro-inflammatory mediators in all treatment groups

	WT	ApoE$^{-/-}$	ApoE$^{-/-}$ + CTS-15	ApoE$^{-/-}$ + CTS-45
IL-1β (pg mL^{-1})	49.6 ± 5.1	286.6 ± 13.3$^{###}$	212.6 ± 10.6**	109.3 ± 6.9***
IL-6 (pg mL^{-1})	5.4 ± 0.1	47.1 ± 2.5$^{###}$	27.9 ± 1.2***	12.8 ± 0.7***
IL-17A (pg mL^{-1})	86.7 ± 5.2	288.3 ± 11.6$^{###}$	222.3 ± 9.9*	140.5 ± 6.3***
IFN-γ (pg mL^{-1})	18.2 ± 0.1	31.3 ± 1.8$^{##}$	23.9 ± 1.2*	19.5 ± 1.0**
TNF-α (pg mL^{-1})	157.5 ± 7.5	443.8 ± 18.4$^{###}$	412.3 ± 22.1	238.0 ± 12.2***

Data are represented as mean ± SEM. $^{##}P < 0.01$, $^{###}P < 0.001$ compared with WT group (n = 6–10 per group).
*$P < 0.05$. **$P < 0.01$. ***$P < 0.001$ compared with ApoE$^{-/-}$ group (treated with vehicle control).

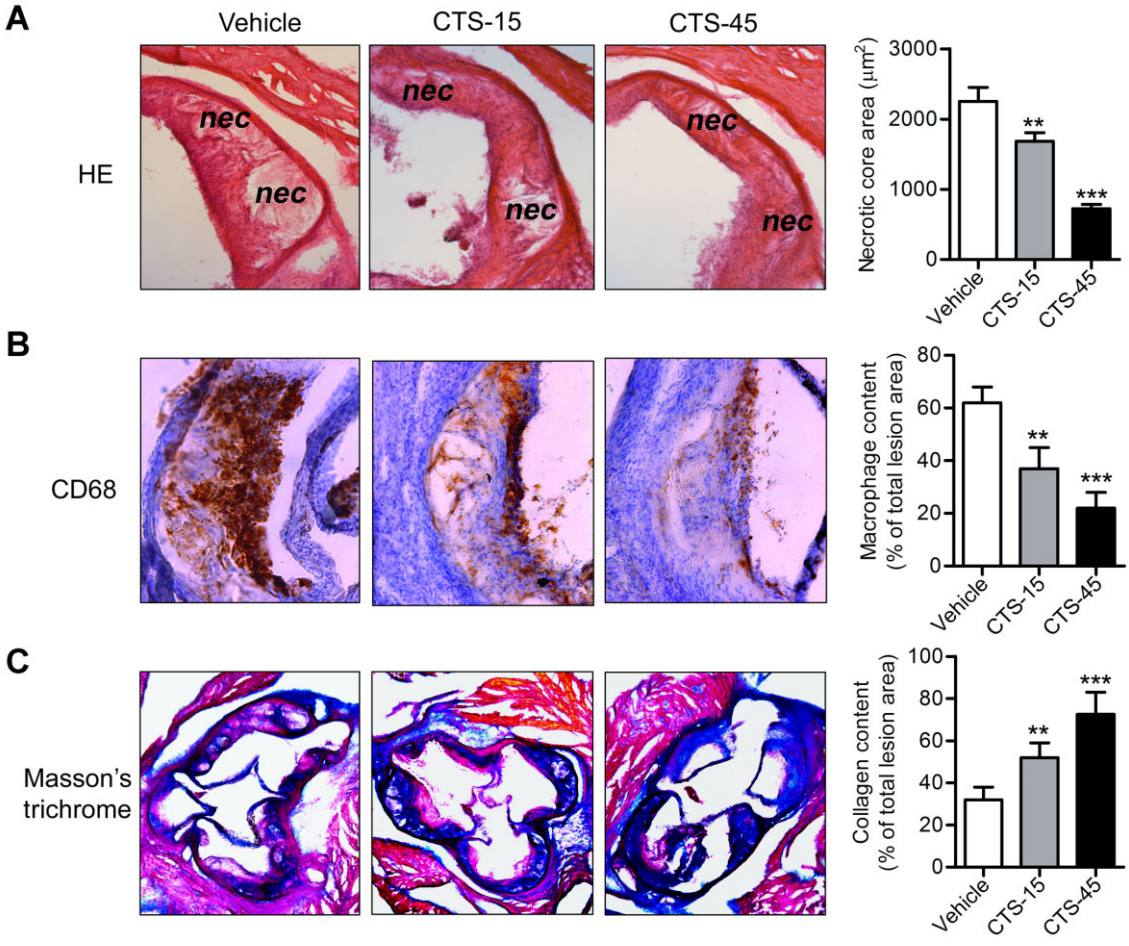

Figure 2

CTS induces features of atherosclerotic plaque stability in ApoE$^{-/-}$ mice. Photomicrographs of sectioned aortic sinus were stained with H&E to calculate necrotic core area (panel A, original magnification, ×100) or immunohistochemically stained for macrophage deposition (CD68 positive, panel B, original magnification, ×100), and collagen content (indicated in blue colour with Masson's trichrome staining, panel C, original magnification, ×50). Corresponding positive areas (CD68 and collagen content) were analysed and quantified using Image-Pro Plus 6.0 software and the percentages of the above plaque components in the entire plaque were evaluated. n = 6 for each group. **$P < 0.01$, ***$P < 0.001$ compared with vehicle group respectively.

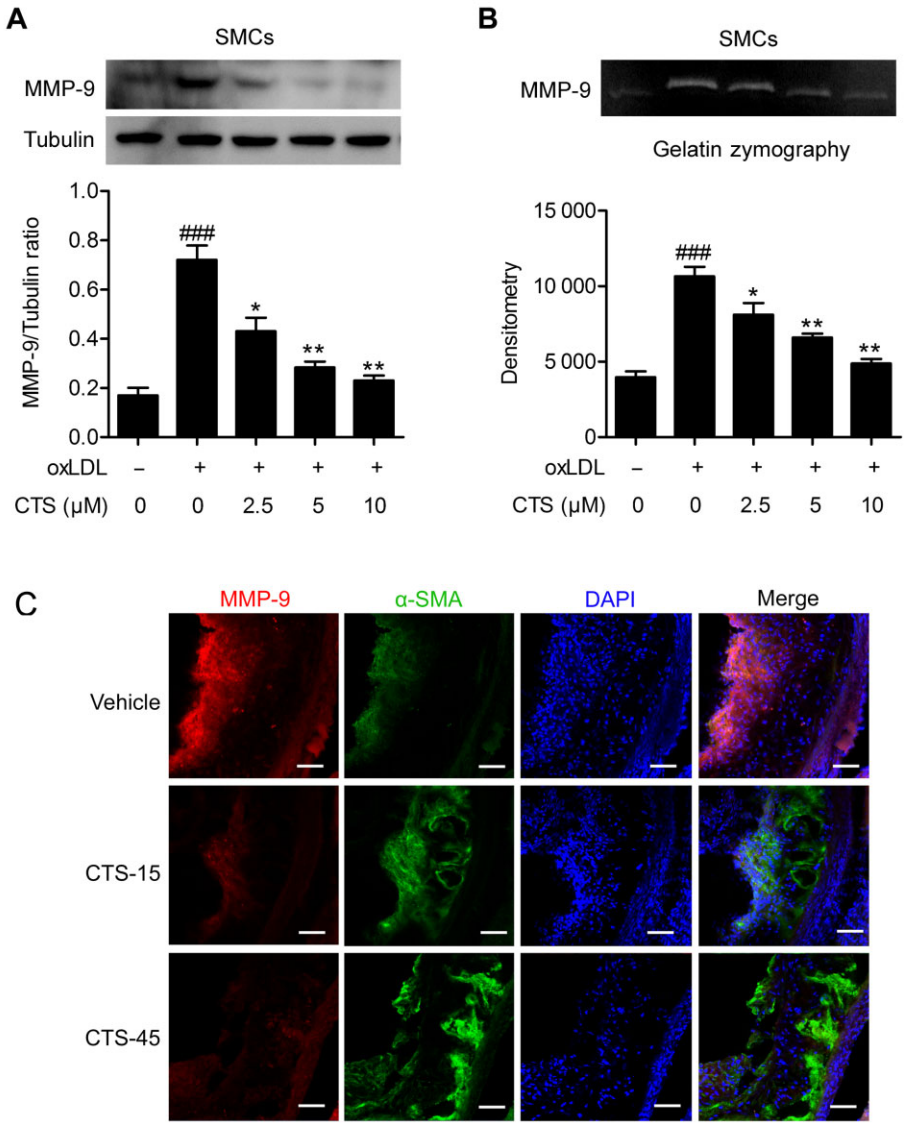

Figure 3

CTS reduces MMP-9 expression and activity. Effect of CTS on oxLDL-stimulated MMP-9 expression and activity in SMCs. Rat aortic SMCs were pretreated with CTS for 3 h then stimulated with oxLDL (80 μg mL^{-1}) for 24 h. Whole cell lysates were subjected to MMP-9 protein expression (A). The conditioned medium from each treatment group was collected and subject to gelatin zymography (B). $n = 6$. $^{###}P < 0.001$ compared with untreated control group; $^{*}P < 0.05$, $^{**}P < 0.01$ compared with oxLDL-treated group respectively. (C) MMP-9 immunohistochemical staining (red) of aortic sinus from ApoE$^{-/-}$ mice receiving CTS or vehicle treatment. SMCs were stained with α-SMA (green) and nuclei were stained with 4′,6-diamidino-2-phenylindole (DAPI) (blue). Scale bar, 50 μm. $n = 8$ for each group.

activity of MMP-9 in oxLDL-treated macrophages (data not shown). However, in SMCs, treatment with CTS significantly decreased MMP-9 protein expression and activity induced by oxLDL in a dose-dependent manner (Figure 3A and B). Consistent with these results, immunohistochemical analysis showed that the expression of MMP-9 was reduced in lesional SMCs within atherosclerotic plaques from CTS-treated ApoE$^{-/-}$ mice compared with vehicle-treated mice (Figure 3C). Moreover, the α-SMA-positive area in atherosclerotic plaques was significantly increased in the CTS treatment group (Figure 3C).

CTS inhibits LOX-1 expression, ROS generation and NF-κB activation in ApoE$^{-/-}$ mice

LOX-1 is a critical scavenger receptor implicated in the initiation and progression of atherosclerosis (Xu *et al.*, 2013b). We next determined whether CTS protects against atherosclerosis by inhibiting LOX-1-mediated signalling pathway in ECs. Immunohistochemistry studies in the aortic sinus from vehicle- and CTS-treated ApoE$^{-/-}$ mice suggest that CTS inhibited aortic LOX-1 expression in a dose-related manner

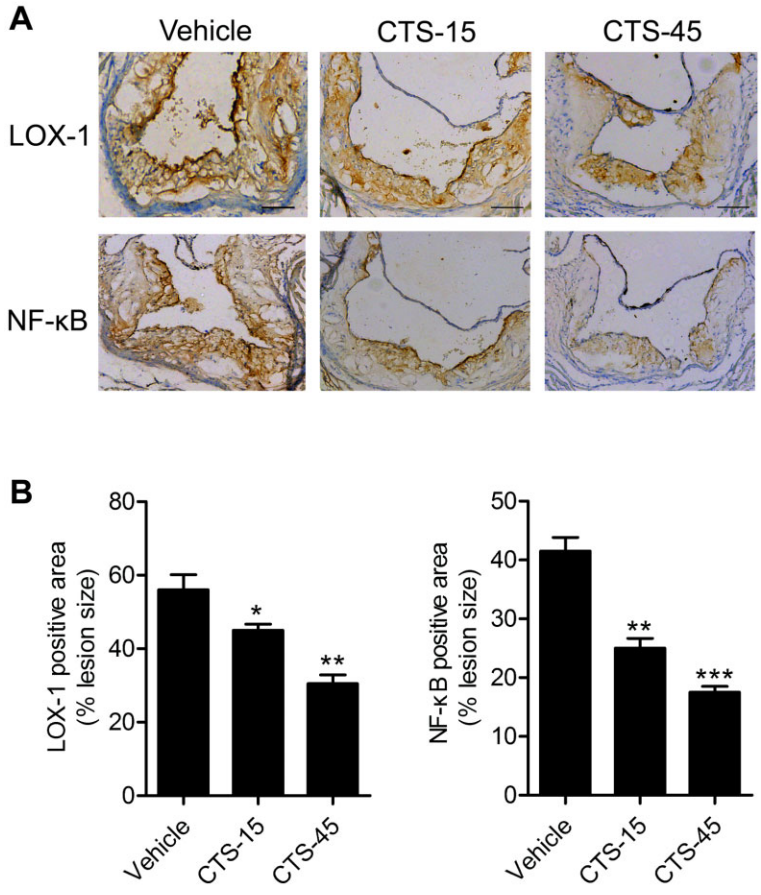

Figure 4

CTS decreases the expression of LOX-1 and NF-κB p65 within the atherosclerotic lesions. (A) Effect of CTS treatment on the expression of LOX-1 and NF-κB p65 in the aorta by immunohistochemistry. (B) Quantitative morphometric analysis of the expression of LOX-1 and NF-κB p65 relative to total plaque size. n = 8–10 for each group. *P < 0.05, **P < 0.01, ***P < 0.001 compared with vehicle group respectively.

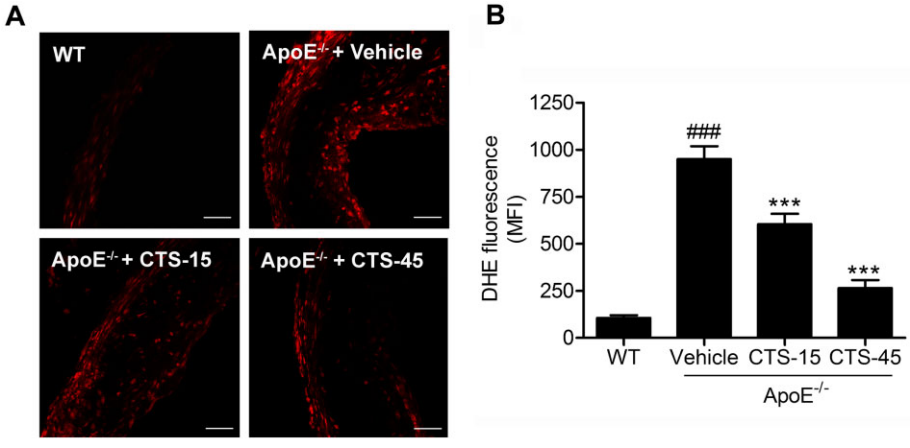

Figure 5

CTS reduces vascular superoxide anion production in aortic vessels from ApoE$^{-/-}$ mice. (A) Representative fluorescent photomicrographs of confocal microscopy of sections labelled with oxidative dye DHE; scale bar, 50 μm. (B) Quantitative analysis of *in situ* superoxide anion production. n = 6–8 for each group. $^{###}P$ < 0.001 compared with wild-type group, ***P < 0.001 compared with vehicle group.

(Figure 4, CTS-15 group, *$P < 0.05$; CTS-45 group, **$P < 0.01$ respectively). Further analysis of *in situ* generation of ROS by DHE staining suggested that CTS significantly inhibited ROS generation (Figure 5). Moreover, immunostaining analysis indicated that the activation of NF-κB was markedly increased in the aortic sections from ApoE$^{-/-}$ mice fed a HCD and this activation was significantly inhibited by CTS in a dose-dependent manner (Figure 4; $P < 0.01$ for CTS-15 group and $P < 0.001$ for CTS-45 group, compared with ApoE$^{-/-}$ group).

CTS inhibits oxLDL-induced LOX-1 expression in HUVECs

Previous studies have demonstrated that oxLDL up-regulates the expression (mRNA and protein) of endothelial LOX-1 (Li and Mehta, 2000a,b; Li *et al.*, 2001; Mehta *et al.*, 2004). To examine the effect of CTS on LOX-1 expression, cells were pretreated with CTS for 3 h before exposure to oxLDL. As shown in Figure 6, incubation of HUVECs with oxLDL (80 μg mL^{-1}) for 24 h increased the mRNA and protein expression of LOX-1, but this increase was attenuated by pretreatment with CTS. The higher concentration of CTS (10 μM) had a more pronounced effect than the lower concentration (2.5 μM) in this regard (Figure 6). Similar results were obtained when TNF-α was used to induce the up-regulation of LOX-1 (Supporting Information Fig. S2), suggesting that CTS has a non-specific inhibitory effect on the expression of LOX-1.

CTS suppresses oxLDL-induced monocytes adhesion to HUVECs

An increase in oxLDL-induced adhesion of monocytes to ECs is a hallmark of early atherogenesis (Kim *et al.*, 1994; Ramos *et al.*, 1999). LOX-1 activation plays an important role in the adhesion of monocytes to ECs (Mitra *et al.*, 2011; Xu *et al.*, 2013b). To determine the biological significance of the inhibitory effect of CTS on LOX-1 expression, we evaluated the adhesion of monocytes to activated ECs. As shown in Figure 7A and B, oxLDL stimulated th eadhesion of THP-1 monocytes to HUVECs; however, this effect was significantly inhibited by CTS treatment in a dose-dependent manner. Mechanistically, the effect of CTS on the surface expression of adhesion molecules on HUVECs exposed to oxLDL was subsequently examined. As shown in Figure 7C and D, the expression levels of ICAM-1 and VCAM-1 were markedly increased in HUVECs after treatment with oxLDL for 24 h but decreased by treatment with CTS in a dose-dependent manner.

CTSCTS inhibits the generation of superoxide radicals and NF-κB activation in HUVECs

Previous studies have shown that LOX-1 expression and activation are associated with the generation of ROS followed by NF-κB activation (Xu *et al.*, 2013b). Therefore, we conducted experiments to examine superoxide radical generation in response to oxLDL and its modulation by CTS in HUVECs. As shown in Figure 8A and B, treatment of cells with oxLDL resulted in a more than doubling of superoxide anion generation ($P < 0.001$ compared with baseline). Pretreatment of cells with CTS (5 and 10 μM) markedly reduced the generation of superoxide radicals ($P < 0.001$ compared with that in cells treated with oxLDL). It is well established that endothelial NADPH oxidase (NOX) is a major source of ROS in ECs and aberrant atherogenic oxLDL levels potently induce the generation of NOX-derived ROS. Figure 8C shows that the level of NOX4, one of the most important NOX subunits in ECs (Ago *et al.*, 2004), was approximately twofold higher in cells treated with oxLDL for 24 h than in untreated cells. This effect was inhibited by pretreatment with CTS in a dose-dependent manner. To determine the intracellular mechanism of the inhibitory effect of CTS on LOX-1, we explored the potential role of the redox-sensitive transcription factor NF-κB as the LOX-1 gene promoter has several putative NF-κB binding sites. We observed that oxLDL activated NF-κB DNA binding activity and transcriptional activity, and these effects were attenuated by CTS treatment (Figure 9A and B). Therefore, our data con-

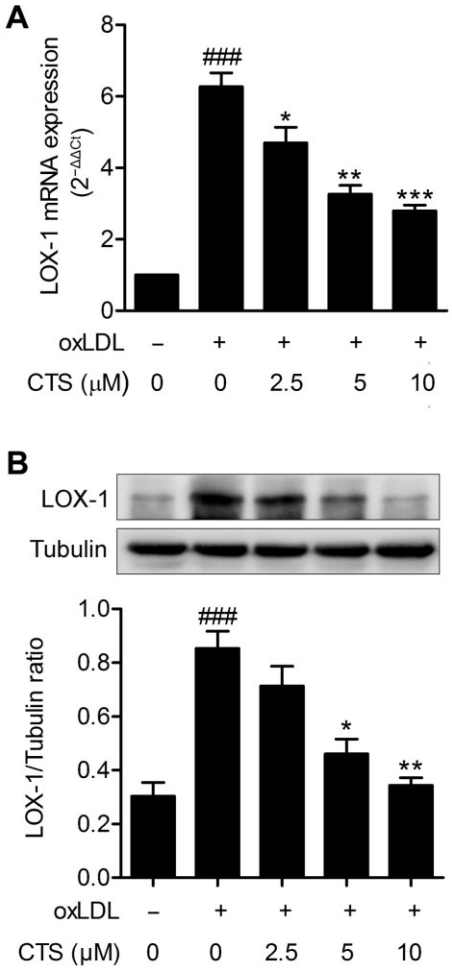

Figure 6

CTS inhibits oxLDL-induced expression of LOX-1 mRNA and protein in HUVECs. HUVECs were pretreated with CTS (2.5–10 μM) for 3 h followed by exposure to oxLDL (80 μg mL^{-1}) for an additional 24 h. At the end of the incubation period cells were lysed, and LOX-1 mRNA (A) and protein (B) were analysed by real-time PCR and Western blot respectively. mRNA levels were quantified versus the GAPDH housekeeping gene. The fold increase versus control cells, calculated by the $2^{-\Delta\Delta Ct}$ method, is shown. $n = 5$. ###$P < 0.001$ compared with untreated control group; *$P < 0.05$, **$P < 0.01$, ***$P < 0.001$ compared with oxLDL-treated group respectively.

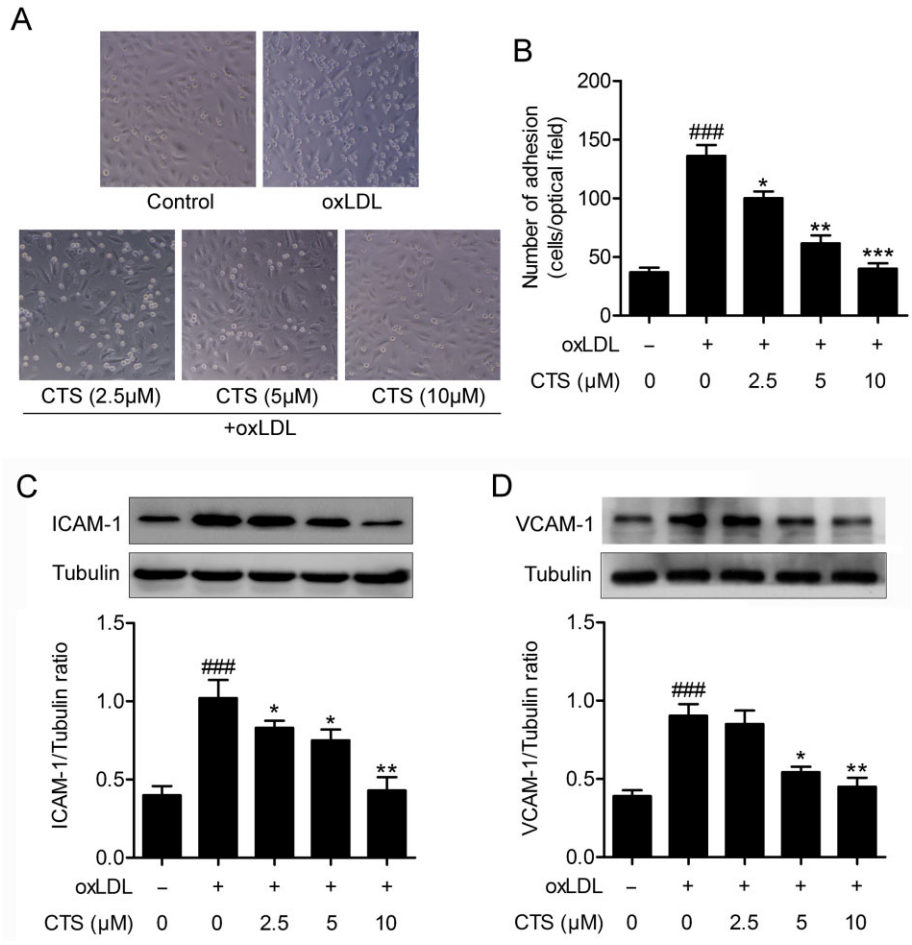

Figure 7

CTS reduces oxLDL-induced expression of adhesion molecules and the adhesion of monocytic cell THP-1 to HUVECs. HUVECs were incubated with the indicated concentrations of CTS for 3 h and then incubated with oxLDL (80 μg mL^{-1}) for an additional 24 h. (A and B) Dose-dependent effect of CTS (2.5–10 μM) on oxLDL-induced adhesion of THP-1 monocytes to HUVECs was measured as described in Methods. $n = 5$. (C and D) Western blot analysis and quantification of ICAM-1 and VCAM-1 protein expression. $n = 6$. $^{###}P < 0.001$, compared with untreated control group; $^{*}P < 0.05$, $^{**}P < 0.01$, $^{***}P < 0.001$ compared with oxLDL-treated group respectively.

vincingly suggest that CTS attenuates the expression of LOX-1 by inhibiting the ROS-NF-κB signalling pathway.

Discussion

In this study, we investigated the effect of CTS on the development of atherosclerosis in HCD-fed ApoE$^{-/-}$ mice, a well-established model for studying atherogenesis. Our data showed that treatment with CTS (15, 45 mg kg^{-1} day^{-1}) resulted in a significant reduction in the size of the atherosclerotic plaque (in aortic sinus and *en face* aorta) and favoured plaque stability (as seen by a reduction in the necrotic core areas and macrophage accumulation, and increased SMC and collagen content), extending observations from previous studies *in vitro* demonstrating the vasculoprotective effects of CTS in macrophages (Don *et al.*, 2007; Tang *et al.*, 2011b), SMCs (Suh *et al.*, 2006; Jin *et al.*, 2009) and ECs (Zhou *et al.*, 2006).

There is increasing evidence that LOX-1, a versatile scavenger receptor that is ubiquitously expressed in vascular cells (ECs, SMCs and macrophages), is critical for the initiation and progression of atherosclerosis (Inoue *et al.*, 2005; Mehta *et al.*, 2007; White *et al.*, 2011). The present study, for the first time, shows the effectiveness of CTS, one of the most abundant lipophilic tanshinones in Danshen at suppressing the expression of LOX-1 within atherosclerotic lesions, suggesting that its anti-atherosclerotic effect is associated with a decrease in the expression of LOX-1. Furthermore, we found that ROS generation and activation of the redox-sensitive NF-κB in the arterial wall was attenuated by CTS treatment, which indicates that the anti-atherogenic effect of CTS is mediated in part through an inhibitory effect on oxidative stress. These *in vivo* observations were repeated in CTS-treated HUVECs stimulated with oxLDL. Moreover, the inhibitory effect of CTS on endothelial LOX-1 expression appears to be exerted at the transcriptional level as reflected by the parallel decrease in LOX-1 mRNA and protein levels in CTS-treated ECs. Previous studies have demonstrated that CTS has pleiotropic effects on cardiovascular and cerebrovascular diseases, neurodegenerative diseases and cancers by regulating several

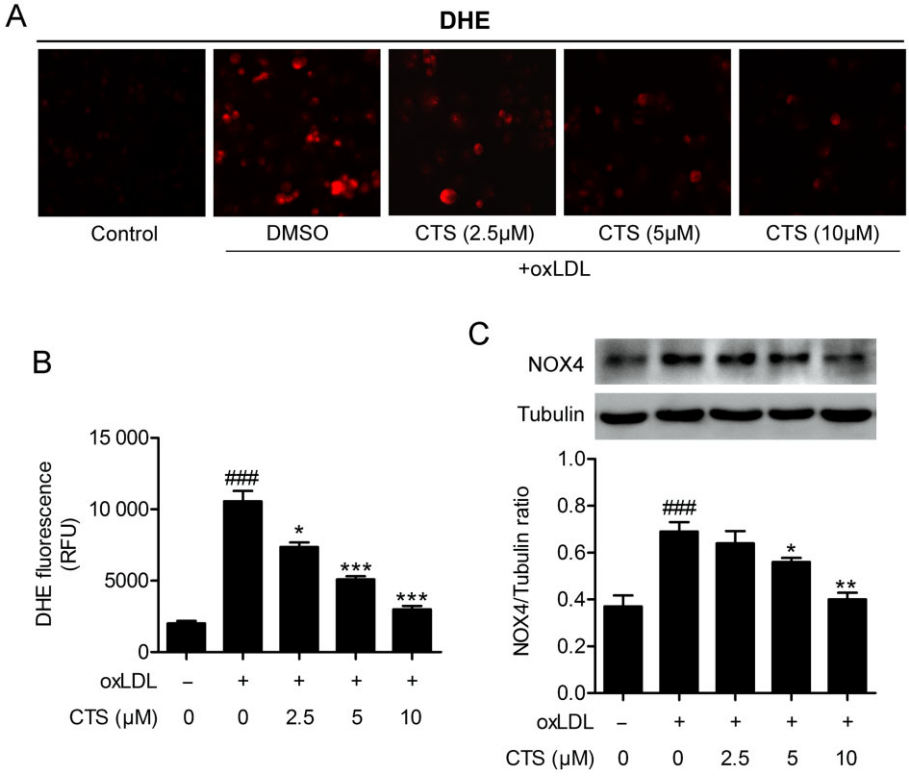

Figure 8

CTS inhibits oxidative stress in HUVECs. HUVECs were pre-incubated with CTS (2.5–10 μM) for 3 h and then exposed to oxLDL (80 μg mL^{-1}) for 2 h. ROS generation was monitored by DHE staining (A) and quantification of superoxide production is shown (B). Western blot analyses and quantification of NOX4 protein expression in HUVECs pretreated with CTS for 3 h followed by 80 μg mL^{-1} oxLDL for 24 h (C). $n = 6$. $^{###}P < 0.001$ compared with untreated control group; $^{*}P < 0.05$, $^{**}P < 0.01$, $^{***}P < 0.001$ compared with oxLDL-treated group respectively.

signalling pathways. Therefore, the beneficial effects of CTS on the development of atherosclerosis may be a combined result of various actions and LOX-1 might be one of the key regulators. One important question that arises from this study and will need to be addressed in the future is whether the protective effects of CTS on atherosclerotic plaque formation are abolished in systemic LOX-1 knockout mice and EC-specific LOX-1 knockout mice. Moreover, considering that Danshen has been widely used in preventing diseases including cardiovascular disorders in humans (Wang *et al.*, 2007; Han *et al.*, 2008), it would be of interest to evaluate the anti-atherosclerotic effect of CTS in atherosclerotic patients.

A major finding of this study is the observation that CTS inhibits ROS production in ECs exposed to oxLDL. The oxLDL-mediated endothelial activation via ROS-induced signal transduction is crucial for endothelial dysfunction in the early phase of atherosclerosis (Li and Mehta, 2000b; Rueckschloss *et al.*, 2001). A recent study found that CTS prevented mitochondrial dysfunction by reducing mitochondrial superoxide production and enhancing mitochondrial SOD activity in hypoxia-induced H9c2 cells (Jin and Li, 2013), suggesting that CTS may have antioxidant properties. It has been shown that ROS can induce the expression of LOX-1 (Cominacini *et al.*, 2000) and LOX-1 activation can in turn stimulate ROS production (Xu *et al.*, 2007), indicating a positive feedback loop between ROS and LOX-1. In this regard, the binding of oxLDL to LOX-1 initiates ROS formation and NF-κB activation, which in turn up-regulates LOX-1 expression and activity, and thus amplifies the vicious cycle of oxLDL. Here, we showed that CTS inhibited oxLDL-induced ROS production and LOX-1 expression in HUVECs, which suggests that the inhibition of LOX-1 expression by CTS might be exerted by reducing ROS generation and blocking the positive feedback loop (Figure 10).

To gain further insight into the mechanism by which CTS inhibits the generation of ROS in HUVECs, we next examined the effect of CTS on NOX4 expression. The NADPH family consists of seven members: NOX1–5, Duox1 and Duox2 (Krause, 2007). Among these, NOX4 expression is 100-fold higher in ECs than in other cell types (Xu *et al.*, 2008), suggesting that NOX4 may play a pivotal role in endothelial ROS generation. In fact, NOX4 is considered to be the predominant NOX subtype in ECs (Ago *et al.*, 2004). The present results showed that CTS attenuated NOX4 expression and ROS production in oxLDL-treated HUVECs, implying that the reduced generation of ROS mediated by CTS is associated with a decrease in the expression of NOX4.

As the regulation of LOX-1 gene expression is redox sensitive and involves NF-κB activation, the suppression of oxLDL-induced ROS production by CTS may contribute to the reduction in LOX-1-mediated activation of NF-κB and subsequent up-regulation of a number of pro-inflammatory

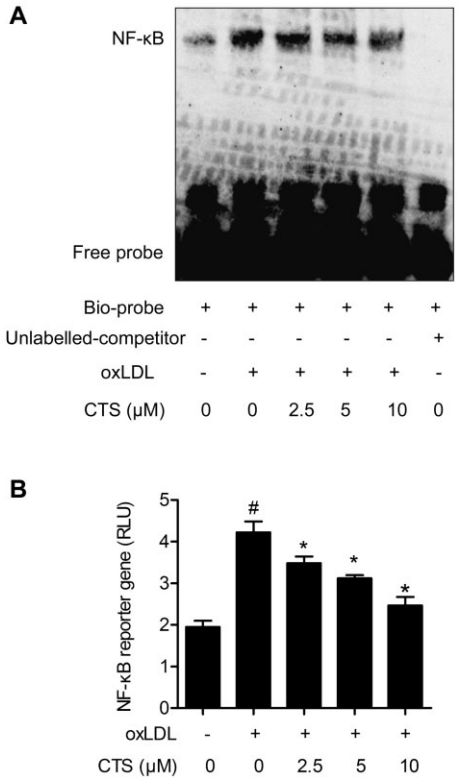

Figure 9

CTS inhibits oxLDL-induced NF-κB DNA binding and transcriptional activity in HUVECs. HUVECs were treated with CTS (2.5–10 μM) for 3 h followed by stimulation with oxLDL (80 μg mL^{-1}) for 24 h. (A) Nuclear extracts (4 μg aliquots) were complexed with a biotin-labelled NF-κB probe and assayed for NF-κB DNA binding activity by EMSA. The specificity of the binding was confirmed by cold competition experiments with a 100-fold molar excess of unlabelled NF-κB duplex oligonucleotide. The graph shows one representative experiment of five independent experiments. (B) Dual luciferase reporter assays were performed to evaluate the influence of CTS treatment on NF-κB-dependent transcriptional activity. Relative luciferase activity was calculated as the ratio of firefly luciferase activity to that of Renilla luciferase. $n = 6$. $^{\#}P < 0.05$ compared with untreated control group; $^{*}P < 0.05$ compared with oxLDL-treated group respectively.

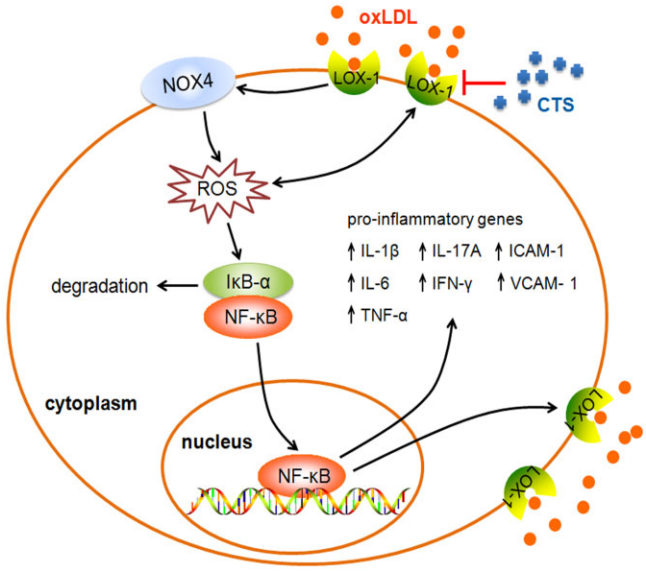

Figure 10

Schematic diagram illustrating the molecular mechanisms underlying the atheroprotective effects of CTS. As depicted, CTS inhibits the LOX-1-mediated signalling cascade to exert its protection against endothelial dysfunction. An arrowhead indicates activation or induction, and a red vertical bar indicates inhibition or blockade.

cytokines and adhesion molecules as well as LOX-1 itself (Figure 10). Therefore, one possible mechanism by which CTS protects against oxLDL-induced endothelial dysfunction is by blocking the LOX-1-mediated signalling pathway, in which binding of oxLDL to LOX-1 activates NOX4 on the cell membrane, resulting in the overproduction of intracellular ROS and the subsequent activation of NF-κB signalling (Figure 10).

Atherosclerosis is a chronic inflammatory and maladaptive immune disease (Libby, 2002; Libby *et al.*, 2011; Moore and Tabas, 2011). There is cumulative evidence suggesting that CTS has a prominent anti-inflammatory effect in macrophages (Jeon *et al.*, 2008; Tang *et al.*, 2011b), ECs (Zhou *et al.*, 2006; Jin *et al.*, 2009), SMCs *in vitro* (Suh *et al.*, 2006) as well as rats and mice *in vivo* (Jin *et al.*, 2009; Tang *et al.*, 2014). In line with these studies, our results showed that CTS inhibits its NF-κB expression in atherosclerotic plaque and reduces the serum levels of pro-inflammatory cytokines in ApoE$^{-/-}$ mice. Previously, we reported that Tanshinone II-A (TSN), another major tanshinone compound isolated from Danshen, possesses anti-atherogenic properties without altering the lipid profile (Xu *et al.*, 2011), which is similar to the results with CTS obtained in the present study. Due to the similar chemical structure, the pharmacokinetic properties of CTS and TSN are also similar (Pan *et al.*, 2008). Therefore, we further compared the effects of CTS and TSN on the expression of LOX-1 and MMP-9, and the results show that CTS is more effective at reducing the expression of LOX-1 and the activity of MMP-9 than TSN (Supporting Information Fig. S3). In comparison with the chemical structure of TSN, CTS has a unique dihydrofuran ring in the C-15 position (Supporting Information Fig. S1), which may contribute to the increased ability of CTS to act as an anti-inflammatory and inhibit the expression of LOX-1 compared to TSN. In a previous study, we found that TSN inhibited the expression of CD36 by inactivating PPARγ and decreasing the uptake of DiI-oxLDL, whereas it did not alter the expression of scavenger receptor-A (SR-A) in macrophages exposed to oxLDL (Tang *et al.*, 2011a). However, recent work from our laboratory has demonstrated that CTS has no significant effect on the internalization of DiI-oxLDL in macrophages (Cheng *et al.*, 2014). Further studies showed that CTS down-regulates CD36 and PPARγ expression but up-regulates SR-A expression in oxLDL-treated macrophages (Supporting Information Fig. S4). Therefore, the effects of CTS on the internalization of Dil-oxLDL may be a combined result of various actions and warrants further investigation.

Taken together, our present results have identified a novel atheroprotective effect of CTS, which was extracted from the traditional Chinese medicine Danshen, and indicated the novel mechanisms by which CTS prevents atherogenesis. CTS

was shown to suppress the ROS/NF-κB signalling pathway, thereby reducing the expression of the endothelial scavenger receptor LOX-1 and diminishing the adhesion of monocytes to ECs. These observations indicate that CTS could be exploited as an innovative cardiovascular drug to prevent or retard the pathogenesis of atherosclerotic cardiovascular diseases.

Acknowledgements

The authors gratefully acknowledge financial support from National Natural Science Foundation of China (no. 81072641 and no. 81273499); the National Science and Technology Major Project of China 'Key New Drug Creation and Manufacturing Program' (no. 2011ZX09401-307). The work was partially supported by grants from the National Institutes of Health (R01HL109502 and R01HL114570 to Z.-G. J.) and the American Diabetes Association (1-12-BS-92-R1 to Z.-G. J.). The authors are very grateful to Professor Michael Curtis (St Thomas' Hospital, London, United Kingdom) and Professor Peter J Little (RMIT University, Melbourne, Australia) for suggestions on statistical analysis.

Author contributions

Z. L., P. L. and S. X. conceived and designed the experiments. Z. L., X. H., J. W., S. G. and H. L. performed the experiments. S. C., J. Y. and Z.-G. J. analysed the data. C. Z. contributed reagents/materials/analysis tools. Z. L. and S. X. wrote the paper.

Conflict of interest

The authors have no conflict of interest to disclose.

References

Ago T, Kitazono T, Ooboshi H, Iyama T, Han YH, Takada J *et al.* (2004). Nox4 as the major catalytic component of an endothelial NAD(P)H oxidase. Circulation 109: 227–233.

Alexander SPH, Benson HE, Faccenda E, Pawson AJ, Sharman JL, Spedding M *et al.* (2013a). The Concise Guide to PHARMACOLOGY 2013/14: Nuclear hormone receptors. Br J Pharmacol. 170: 1652–1675.

Alexander SPH, Benson HE, Faccenda E, Pawson AJ, Sharman JL, Spedding M *et al.* (2013b). The Concise Guide to PHARMACOLOGY 2013/14: Enzymes. Br J Pharmacol. 170: 1797–1867.

Ang KP, Tan HK, Selvaraja M, Kadir AA, Somchit MN, Akim AM *et al.* (2011). Cryptotanshinone attenuates in vitro oxLDL-induced pre-lesional atherosclerotic events. Planta Med 77: 1782–1787.

Besler C, Heinrich K, Rohrer L, Doerries C, Riwanto M, Shih DM *et al.* (2011). Mechanisms underlying adverse effects of HDL on eNOS-activating pathways in patients with coronary artery disease. J Clin Invest 121: 2693–2708.

Chen W, Luo Y, Liu L, Zhou H, Xu B, Han X *et al.* (2010). Cryptotanshinone inhibits cancer cell proliferation by suppressing mammalian target of rapamycin-mediated cyclin D1 expression and Rb phosphorylation. Cancer Prev Res 3: 1015–1025.

Chen W, Tang F, Xie B, Chen S, Huang H, Liu P (2012). Amelioration of atherosclerosis by tanshinone IIA in hyperlipidemic rabbits through attenuation of oxidative stress. Eur J Pharmacol 674: 359–364.

Cheng X, Zhang DL, Li XB, Ye JT, Shi L, Huang ZS *et al.* (2014). Syntheses of diacyltanshinol derivatives and their suppressive effects on macrophage foam cell formation by reducing oxidized LDL uptake. Bioorg Chem 52: 24–30.

Cominacini L, Pasini AF, Garbin U, Davoli A, Tosetti ML, Campagnola M *et al.* (2000). Oxidized low density lipoprotein (ox-LDL) binding to ox-LDL receptor-1 in endothelial cells induces the activation of NF-kappaB through an increased production of intracellular reactive oxygen species. J Biol Chem 275: 12633–12638.

Don MJ, Liao JF, Lin LY, Chiou WF (2007). Cryptotanshinone inhibits chemotactic migration in macrophages through negative regulation of the PI3K signaling pathway. Br J Pharmacol 151: 638–646.

Gao S, Liu Z, Li H, Little PJ, Liu P, Xu S (2012). Cardiovascular actions and therapeutic potential of tanshinone IIA. Atherosclerosis 220: 3–10.

Han JY, Fan JY, Horie Y, Miura S, Cui DH, Ishii H *et al.* (2008). Ameliorating effects of compounds derived from *Salvia miltiorrhiza* root extract on microcirculatory disturbance and target organ injury by ischemia and reperfusion. Pharmacol Ther 117: 280–295.

Inoue K, Arai Y, Kurihara H, Kita T, Sawamura T (2005). Overexpression of lectin-like oxidized low-density lipoprotein receptor-1 induces intramyocardial vasculopathy in apolipoprotein E-null mice. Circ Res 97: 176–184.

Jeon SJ, Son KH, Kim YS, Choi YH, Kim HP (2008). Inhibition of prostaglandin and nitric oxide production in lipopolysaccharide-treated RAW 264.7 cells by tanshinones from the roots of *Salvia miltiorrhiza* bunge. Arch Pharm Res 31: 758–763.

Jin HJ, Li CG (2013). Tanshinone IIA and cryptotanshinone prevent mitochondrial dysfunction in hypoxia-induced H9c2 cells: association to mitochondrial ROS, intracellular nitric oxide, and calcium levels. Evid Based Complement Alternat Med 2013: 610694.

Jin YC, Kim CW, Kim YM, Nizamutdinova IT, Ha YM, Kim HJ *et al.* (2009). Cryptotanshinone, a lipophilic compound of *Salvia miltiorrhiza* root, inhibits TNF-alpha-induced expression of adhesion molecules in HUVEC and attenuates rat myocardial ischemia/reperfusion injury in vivo. Eur J Pharmacol 614: 91–97.

Kataoka H, Kume N, Miyamoto S, Minami M, Moriwaki H, Murase T *et al.* (1999). Expression of lectin like oxidized low-density lipoprotein receptor-1 in human atherosclerotic lesions. Circulation 99: 3110–3117.

Kato R, Mori C, Kitazato K, Arata S, Obama T, Mori M *et al.* (2009). Transient increase in plasma oxidized LDL during the progression of atherosclerosis in apolipoprotein E knockout mice. Arterioscler Thromb Vasc Biol 29: 33–39.

Kilkenny C, Browne W, Cuthill IC, Emerson M, Altman DG (2010). Animal research: reporting *in vivo* experiments: the ARRIVE guidelines. Br J Pharmacol 160: 1577–1579.

Kim EJ, Jung SN, Son KH, Kim SR, Ha TY, Park MG *et al.* (2007). Antidiabetes and antiobesity effect of cryptotanshinone via activation of AMP-activated protein kinase. Mol Pharmacol 72: 62–72.

Kim JA, Territo MC, Wayner E, Carlos TM, Parhami F, Smith CW *et al*. (1994). Partial characterization of leukocyte binding molecules on endothelial cells induced by minimally oxidized LDL. Arterioscler Thromb 14: 427–433.

Krause KH (2007). Aging: a revisited theory based on free radicals generated by NOX family NADPH oxidases. Exp Gerontol 42: 256–262.

Li AC, Glass CK (2002). The macrophage foam cell as a target for therapeutic intervention. Nat Med 8: 1235–1242.

Li D, Mehta JL (2000a). Upregulation of endothelial receptor for oxidized LDL (LOX-1) by oxidized LDL and implications in apoptosis of human coronary artery endothelial cells: evidence from use of antisense LOX-1 mRNA and chemical inhibitors. Arterioscler Thromb Vasc Biol 20: 1116–1122.

Li D, Mehta JL (2000b). Antisense to LOX-1 inhibits oxidized LDL-mediated upregulation of monocyte chemoattractant protein-1 and monocyte adhesion to human coronary artery endothelial cells. Circulation 101: 2889–2895.

Li D, Mehta JL (2009). Intracellular signaling of LOX-1 in endothelial cell apoptosis. Circ Res 104: 566–568.

Li D, Liu L, Chen H, Sawamura T, Ranganathan S, Mehta JL (2003). LOX-1 mediates oxidized low-density lipoprotein-induced expression of matrix metalloproteinases in human coronary artery endothelial cells. Circulation 107: 612–617.

Li DY, Chen HJ, Mehta JL (2001). Statins inhibit oxidized-LDL-mediated LOX-1 expression, uptake of oxidized-LDL and reduction in PKB phosphorylation. Cardiovasc Res 52: 130–135.

Libby P (2002). Inflammation in atherosclerosis. Nature 420: 868–874.

Libby P, Ridker PM, Hansson GK (2011). Progress and challenges in translating the biology of atherosclerosis. Nature 473: 317–325.

Libby P, Lichtman AH, Hansson GK (2013). Immune effector mechanisms implicated in atherosclerosis: from mice to humans. Immunity 38: 1092–1104.

Liu Z, Wang J, Huang E, Gao S, Li H, Lu J *et al*. (2014). Tanshinone IIA suppresses cholesterol accumulation in human macrophages: role of heme oxygenase-1. J Lipid Res 55: 201–213.

Livak KJ, Schmittgen TD (2001). Analysis of relative gene expression data using real-time quantitative PCR and the 2(-Delta Delta C(T)) method. Methods 25: 402–408.

McGrath J, Drummond G, McLachlan E, Kilkenny C, Wainwright C (2010). Guidelines for reporting experiments involving animals: the ARRIVE guidelines. Br J Pharmacol 160: 1573–1576.

Mehta JL, Chen J, Yu F, Li DY (2004). Aspirin inhibits ox-LDL-mediated LOX-1 expression and metalloproteinase-1 in human coronary endothelial cells. Cardiovasc Res 64: 243–249.

Mehta JL, Sanada N, Hu CP, Chen J, Dandapat A, Sugawara F *et al*. (2007). Deletion of LOX-1 reduces atherogenesis in LDLR knockout mice fed high cholesterol diet. Circ Res 100: 1634–1642.

Mei Z, Zhang F, Tao L, Zheng W, Cao Y, Wang Z *et al*. (2009). Cryptotanshinone, a compound from *Salvia miltiorrhiza* modulates amyloid precursor protein metabolism and attenuates beta-amyloid deposition through upregulating alpha-secretase in vivo and in vitro. Neurosci Lett 452: 90–95.

Mei Z, Yan P, Situ B, Mou Y, Liu P (2012). Cryptotanshinone inhibits beta-amyloid aggregation and protects damage from beta-amyloid in SH-SY5Y cells. Neurochem Res 37: 622–628.

Mitra S, Goyal T, Mehta JL (2011). Oxidized LDL, LOX-1 and atherosclerosis. Cardiovasc Drugs Ther 25: 419–429.

Moore KJ, Tabas I (2011). Macrophages in the pathogenesis of atherosclerosis. Cell 145: 341–355.

Pan Y, Bi HC, Zhong GP, Chen X, Zuo Z, Zhao LZ *et al*. (2008). Pharmacokinetic characterization of hydroxylpropyl-beta-cyclodextrin-included complex of cryptotanshinone, an investigational cardiovascular drug purified from Danshen (*Salvia miltiorrhiza*). Xenobiotica 38: 382–398.

Pawson AJ, Sharman JL, Benson HE, Faccenda E, Alexander SP, Buneman OP *et al*.; NC-IUPHAR (2014). The IUPHAR/BPS Guide to PHARMACOLOGY: an expert-driven knowledgebase of drug targets and their ligands. Nucl. Acids Res. 42 (Database Issue): D1098–106.

Ramos CL, Huo Y, Jung U, Ghosh S, Manka DR, Sarembock IJ *et al*. (1999). Direct demonstration of P-selectin- and VCAM-1-dependent mononuclear cell rolling in early atherosclerotic lesions of apolipoprotein E-deficient mice. Circ Res 84: 1237–1244.

Ross R (1999). Atherosclerosis – an inflammatory disease. N Engl J Med 340: 115–126.

Rueckschloss U, Galle J, Holtz J, Zerkowski HR, Morawietz H (2001). Induction of NAD(P)H oxidase by oxidized low-density lipoprotein in human endothelial cells: antioxidative potential of hydroxymethylglutaryl coenzyme A reductase inhibitor therapy. Circulation 104: 1767–1772.

Sawamura T, Kume N, Aoyama T, Moriwaki H, Hoshikawa H, Aiba Y *et al*. (1997). An endothelial receptor for oxidized low-density lipoprotein. Nature 386: 73–77.

Shin DS, Kim HN, Shin KD, Yoon YJ, Kim SJ, Han DC *et al*. (2009). Cryptotanshinone inhibits constitutive signal transducer and activator of transcription 3 function through blocking the dimerization in DU145 prostate cancer cells. Cancer Res 69: 193–202.

Suh SJ, Jin UH, Choi HJ, Chang HW, Son JK, Lee SH *et al*. (2006). Cryptotanshinone from *Salvia miltiorrhiza* BUNGE has an inhibitory effect on TNF-alpha-induced matrix metalloproteinase-9 production and HASMC migration via down-regulated NF-kappaB and AP-1. Biochem Pharmacol 72: 1680–1689.

Tang F, Wu X, Wang T, Wang P, Li R, Zhang H *et al*. (2007). Tanshinone II A attenuates atherosclerotic calcification in rat model by inhibition of oxidative stress. Vascul Pharmacol 46: 427–438.

Tang FT, Cao Y, Wang TQ, Wang LJ, Guo J, Zhou XS *et al*. (2011a). Tanshinone IIA attenuates atherosclerosis in ApoE(–/–) mice through down-regulation of scavenger receptor expression. Eur J Pharmacol 650: 275–284.

Tang S, Shen XY, Huang HQ, Xu SW, Yu Y, Zhou CH *et al*. (2011b). Cryptotanshinone suppressed inflammatory cytokines secretion in RAW264.7 macrophages through inhibition of the NF-kappaB and MAPK signaling pathways. Inflammation 34: 111–118.

Tang Y, Chen Y, Chu Z, Yan B, Xu L (2014). Protective effect of cryptotanshinone on lipopolysaccharide-induced acute lung injury in mice. Eur J Pharmacol 723: 494–500.

Wang X, Morris-Natschke SL, Lee KH (2007). New developments in the chemistry and biology of the bioactive constituents of Tanshen. Med Res Rev 27: 133–148.

White SJ, Sala-Newby GB, Newby AC (2011). Overexpression of scavenger receptor LOX-1 in endothelial cells promotes atherogenesis in the ApoE(–/–) mouse model. Cardiovasc Pathol 20: 369–373.

Xu H, Goettsch C, Xia N, Horke S, Morawietz H, Forstermann U *et al*. (2008). Differential roles of PKCalpha and PKCepsilon in

controlling the gene expression of Nox4 in human endothelial cells. Free Radic Biol Med 44: 1656–1667.

Xu S, Liu P (2013a). Tanshinone II-A: new perspectives for old remedies. Expert Opin Ther Pat 23: 149–153.

Xu S, Fu J, Chen J, Xiao P, Lan T, Le K *et al.* (2009). Development of an optimized protocol for primary culture of smooth muscle cells from rat thoracic aortas. Cytotechnology 61: 65–72.

Xu S, Little PJ, Lan T, Huang Y, Le K, Wu X *et al.* (2011). Tanshinone II-A attenuates and stabilizes atherosclerotic plaques in apolipoprotein-E knockout mice fed a high cholesterol diet. Arch Biochem Biophys 515: 72–79.

Xu S, Liu Z, Huang Y, Le K, Tang F, Huang H *et al.* (2012). Tanshinone II-A inhibits oxidized LDL-induced LOX-1 expression in macrophages by reducing intracellular superoxide radical generation and NF-kappaB activation. Transl Res 160: 114–124.

Xu S, Ogura S, Chen J, Little PJ, Moss J, Liu P (2013b). LOX-1 in atherosclerosis: biological functions and pharmacological modifiers. Cell Mol Life Sci 70: 2859–2872.

Xu X, Gao X, Potter BJ, Cao JM, Zhang C (2007). Anti-LOX-1 rescues endothelial function in coronary arterioles in atherosclerotic ApoE knockout mice. Arterioscler Thromb Vasc Biol 27: 871–877.

Yu SS, Cai Y, Ye JT, Pi RB, Chen SR, Liu PQ *et al.* (2013). Sirtuin 6 protects cardiomyocytes from hypertrophy in vitro via inhibition of NF-kappaB-dependent transcriptional activity. Br J Pharmacol 168: 117–128.

Zhou Z, Wang SQ, Liu Y, Miao AD (2006). Cryptotanshinone inhibits endothelin-1 expression and stimulates nitric oxide production in human vascular endothelial cells. Biochim Biophys Acta 1760: 1–9.

Supporting information

Additional Supporting Information may be found in the online version of this article at the publisher's web-site:

http://dx.doi.org/10.1111/bph.13068

Figure S1 The chemical structures of cryptotanshinone (CTS) and tanshinone IIA (TSN).
Figure S2 Inhibitory effect of CTS on TNF-α-induced LOX-1 expression.
Figure S3 Effect of CTS and TSN on oxLDL-stimulated LOX-1 and MMP-9 expression.
Figure S4 Effect of CTS on mRNA expression of SR-A, CD36 and PPARγ in macrophages treated with oxLDL.
Table S1 Primer sets used for real-time PCR.
Table S2 Serum lipid profile in all treatment groups.